Microsc. Microanal. 19, S5, 149–151, 2013
doi:10.1017/S1431927613012531

Microstructural Analysis of Dehydrogenation Products of the $Ca(BH_4)_2$–MgH_2 Composite

Jong-Min Kim,[1] Yoonyoung Kim,[2] Jae-Hyeok Shim,[2] Young-Su Lee,[2] Jin-Yoo Suh,[2,*] Jae-Pyoung Ahn,[1] Gyeung-Ho Kim,[1] and Young Whan Cho[2]

[1]*Advanced Analysis Center, Korea Institute of Science and Technology, Seoul 136-791, Republic of Korea*
[2]*High Temperature Energy Materials Research Center, Korea Institute of Science and Technology, Seoul 136-791, Republic of Korea*

Abstract: The microstructural analysis of the dehydrogenation products of the $Ca(BH_4)_2$–MgH_2 composite was performed using transmission electron microscopy. It was found that nanocrystalline CaB_6 crystallites formed as a dehydrogenation product throughout the areas where the signals of Ca and Mg were simultaneously detected, in addition to relatively coarse Mg crystallites. The uniform distribution of the nanocrystalline CaB_6 crystallites appears to play a key role in the rehydrogenation of the dehydrogenation products, which implies that microstructure is a crucial factor determining the reversibility of reactive hydride composites.

Key words: solid-state hydrogen storage, complex hydride, dehydrogenation reaction, rehydrogenation reaction, reversibility, air sensitivity, air-lock transfer, transmission electron microscopy

Introduction

Metal borohydrides such as $LiBH_4$, $Ca(BH_4)_2$, and $Mg(BH_4)_2$ have been regarded as promising candidates for solid-state hydrogen storage materials, because they have high gravimetric hydrogen storage densities (Orimo et al., 2007). However, their high dehydrogenation temperature and poor reversibility for the dehydrogenation and rehydrogenation reactions are serious drawbacks. To mitigate these drawbacks, the concept of reactive hydride composite such as $LiBH_4$–MgH_2 has been devised (Vajo et al., 2005; Barkhordarian et al., 2007; Bösenberg et al., 2007), in which the composite releases hydrogen by a mutual reaction between metal borohydride and metal hydride.

$Ca(BH_4)_2$ is known to be dehydrogenated into CaH_2 and CaB_6, releasing 9.6 wt% H_2. The rehydrogenation of CaH_2 and CaB_6 into $Ca(BH_4)_2$ was also achieved at relatively moderate pressure and temperature conditions with the help of catalytic additives, although it was not complete (Kim et al., 2008*a*, 2008*b*; Rongeat et al., 2010). Recently, the dehydrogenation and rehydrogenation behavior of the $Ca(BH_4)_2$–MgH_2 composite has been investigated (Kim et al., 2009). X-ray diffraction and Raman spectroscopy showed that the composite was finally dehydrogenated into CaH_2, CaB_6, and Mg through a couple of intermediate stages, based on the following reaction:

$$Ca(BH_4)_2 + MgH_2 \rightarrow 2/3CaH_2 + 1/3CaB_6 + Mg + 13/3H_2\ (9.1\ wt\%H_2). \quad (1)$$

In addition, about 60% reversibility was confirmed after the rehydrogenation at 350°C and 90 bar H_2 without any catalytic additive. However, the microstructural analysis of this composite has never been carried out, in spite of the importance of microstructure in controlling the dehydrogenation and rehydrogenation reactions of reactive hydride composites (Kim et al., 2010).

In this study, we performed the microstructural analysis of the dehydrogenation products of the $Ca(BH_4)_2$–MgH_2 composite using transmission electron microscopy (TEM) and focused ion beam (FIB) milling. Special interest was paid to the size and distribution of CaB_6 crystallites, and their role in the rehydrogenation reaction was briefly discussed.

Materials and Methods

A mixture of $Ca(BH_4)_2$ and MgH_2 powders with a molar ratio of 1:1 was prepared from $Ca(BH_4)_2$ (assay 98%, Sigma-Aldrich) and MgH_2 (assay 98%, Alfa Aesar) using ball milling (Fritsch P7). The dehydrogenation of the composite was conducted at 400°C under static vacuum. The details of the sample preparation procedure can be found in Kim et al. (2009).

Owing to the air sensitivity of $Ca(BH_4)_2$ and MgH_2, the sample was handled inside an Ar-filled glove box (Woosung Hi-Vac) where water and oxygen levels were kept below 1 ppm. The TEM samples were prepared by an FEI Qunata3D FIB equipped with a Gatan Alto transfer system for the air-lock transfer of the samples. A Gatan double-tilt vacuum transfer TEM holder, model 648, was used for the sample transfer into a TEM. The TEM observations were performed using FEI Tecnai F20 and Titan TEMs.

Results and Discussion

A low-magnification bright-field TEM image showing a wide area of the dehydrogenated sample prepared by the FIB milling is given in Figure 1a. Figure 1b shows a magnified high-angle annular dark-field (HAADF) image of the

*Corresponding author. E-mail: jinyoo@kist.re.kr

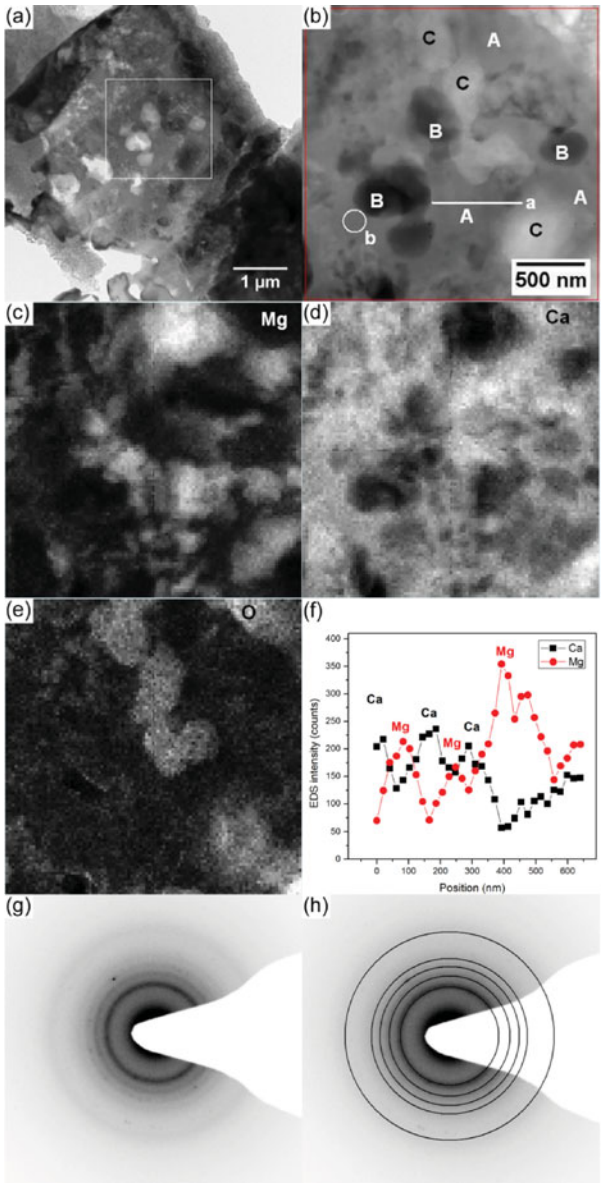

Figure 1. **a**: Low-magnification image of the specimen. **b**: High-angle annular dark-field image of the area marked by a square in (**a**). Maps showing elemental distribution of (**c**) Mg, (**d**) Ca, and (**e**) O acquired by EDS mapping on the area shown in (**b**). (**f**) Line profile of energy-dispersive spectroscopy intensity counts of Ca and Mg along the line 'a' defined in (**b**). **g**: Selected area electron diffraction (SAED) pattern of the area defined by the circle 'b' of (**b**). **h**: SAED pattern (**g**) superposed by the ring pattern of {110}, {111}, {200}, {210}, and {300} diffractions of the CaB_6 crystal structure.

area in the square in Figure 1a. The dark areas marked with B's in Figure 1b are holes or very thin areas, as the HAADF mode constructs image contrast mostly by atomic number difference, so-called Z-contrast. The bright areas marked with C's seem to be oxide impurities, as shown in Figure 1e. On the other hand, Ca and Mg are simultaneously detected in the gray areas marked with A's, as shown in Figures 1c and 1d. Along the line 'a' in Figure 1b, the concentration of Ca and Mg exhibits an oscillating pattern, as shown in Figure 1f. These areas seem to contain both Mg and Ca, Mg- and Ca-rich phases being uniformly mixed in about 100 nm scale. Figure 1g shows a selected area electron diffraction (SAED) pattern on the gray area marked by the circle 'b' in Figure 1b. This pattern agrees with the ring pattern of {110}, {111}, {200}, {210}, and {300} diffractions of the CaB_6 crystal structure [$Pm\bar{3}m(211)$, $a = 4.154$ Å]. There is no evidence of the presence of CaH_2 in these areas, which implies that either CaH_2 or dehydrogenated Ca might exist in the amorphous state. Although the CaH_2 is expected to exist in the dehydrogenation products of the composite, dehydrogenated Ca might exist instead of CaH_2 during the actual TEM observation, owing to an extremely high vacuum level inside TEMs.

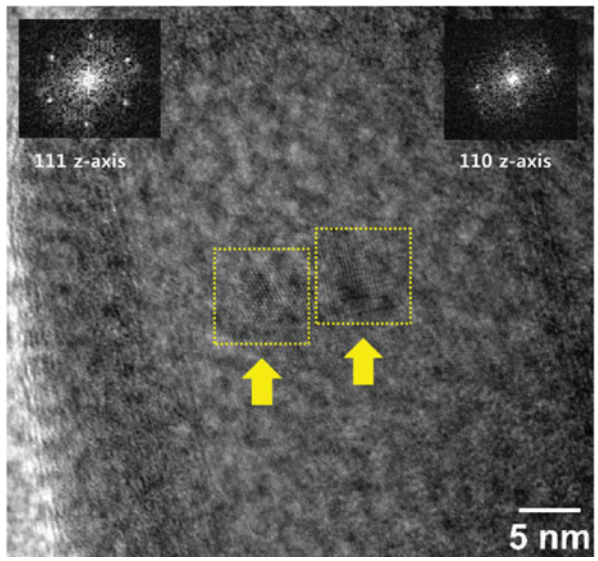

Figure 2. CaB_6 crystallites existing inside the area where the amorphous Ca- and Mg-rich phases are uniformly mixed.

Figure 2 presents a high-resolution image showing two CaB_6 nanocrystallites aligned with the [111] and [110] zone axes. Those nanocrystallites are surrounded by an amorphous matrix containing Mg and Ca. From the high-resolution image, the size of the CaB_6 crystallites is estimated at about 5 nm. Figures 1g and 2 confirm that CaB_6 exists in the form of nanocrystallites throughout the areas where amorphous Mg- and Ca-rich phases are mixed together.

On the other hand, relatively coarse crystallites of pure Mg are also found. For example, the dark area marked by the white circle in Figure 3a turns out to be pure Mg as confirmed by the diffraction pattern shown in Figure 3b. The diffraction pattern exhibits the [311] zone axis of pure hexagonal close-packed Mg. These are different from the Mg-rich phases mixed with the Ca-rich phases shown in Figures 1 and 2, which exist in the form of amorphous structure. Those coarse Mg crystallites (size of the order of 100 nm) appear to be the dehydrogenation product of isolated MgH_2, which was not mixed with $Ca(BH_4)_2$.

According to Kim et al. (2009, 2010), the dehydrogenation process of the $Ca(BH_4)_2 + MgH_2$ composite starts with the dehydrogenation of MgH_2, followed by the formation of

https://doi.org/10.1017/S1431927613012531 Published online by Cambridge University Press

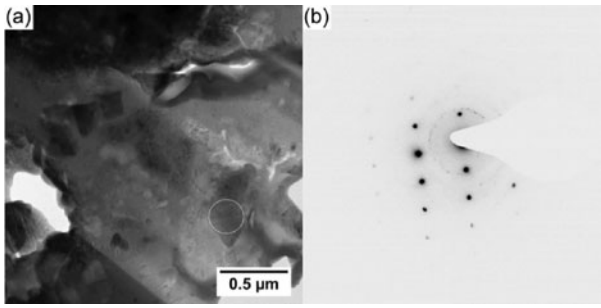

Figure 3. a: Low-magnification image of the specimen area containing relatively coarse crystallites of pure Mg. **b:** Selected area electron diffraction pattern of the area defined by the circle in (**a**) showing Mg [311] zone diffraction pattern.

the intermediate phase, $Ca_4Mg_3H_{14}$. $Ca_4Mg_3H_{14}$ is eventually decomposed into CaH_2 and Mg during the dehydrogenation. The decomposition of the intermediate phase is thought to be responsible for the formation of the regions mixed with Ca- and Mg-rich amorphous phases in the scale of the order of 100 nm.

To confirm the microstructural effect on the rehydrogenation of the composite, the hydrogenation of a ball-milled mixture of CaH_2, CaB_6, and Mg with the molar ratio corresponding to reaction (1) was attempted at 350°C and 90 bar H_2. The considerable hydrogenation of the mixture into $Ca(BH_4)_2$ + MgH_2 was not observed, whereas about 60% reversibility was achieved for the dehydrogenation products at the same condition as mentioned above. The hydrogenation products of the mixture turned out to be $Ca_4Mg_3H_{14}$ and CaB_6 by X-ray diffraction. The size of CaB_6 in the mixture turned out to be in a range between 100 and 400 nm, which is in contrast with that of CaB_6 in the dehydrogenation products (~5 nm). Therefore, it can be concluded that the size of CaB_6 plays a key role in the rehydrogenation of the composite. The very fine size of CaB_6 in the dehydrogenation products is likely to contribute to the rehydrogenation by reducing the distance of long-range diffusion that is required for the rehydrogenation reaction. However, a further study needs to be performed to elucidate whether there is the contribution of the thermodynamic and strain effects, as well as the kinetic effect.

Conclusions

The microstructure of the dehydrogenation products of the $Ca(BH_4)_2$–MgH_2 composite was investigated using TEM. SAED patterns and high-resolution lattice images confirmed the presence of CaB_6 nanocrystallites of about 5 nm size throughout the areas where the amorphous Ca- and Mg-rich phases are uniformly mixed. The formation of the areas seems to be attributed to the decomposition of the intermediate phase $Ca_4Mg_3H_{14}$. The very fine size of the CaB_6 crystallites is likely to play a key role in the rehydrogenation of the composite.

Acknowledgment

This study was supported by Korea Institute of Science and Technology (2E24022 and 2E24043).

References

Barkhordarian, G., Klassen, T., Dornheim, M. & Bormann, R. (2007). Unexpected kinetic effect of MgB_2 in reactive hydride composites containing complex borohydrides. *J Alloy Compd* **440**(1–2), L18–L21.

Bösenberg, U., Doppiu, S., Mosegaard, L., Barkhordarian, G., Eigen, N., Borgschulte, A., Jensen, T.R., Cerenius, Y., Gutfleisch, O., Klassen, T., Dornheim, M. & Bormann, R. (2007). Hydrogen sorption properties of MgH_2–$LiBH_4$ composites. *Acta Mater* **55**(11), 3951–3958.

Kim, J.H., Jin, S.A., Shim, J.H. & Cho, Y.W. (2008*a*). Reversible hydrogen storage in calcium borohydride $Ca(BH_4)_2$. *Scr Mater* **58**(6), 481–483.

Kim, J.H., Shim, J.H. & Cho, Y.W. (2008*b*). On the reversibility of hydrogen storage in Ti- and Nb-catalyzed $Ca(BH_4)_2$. *J Power Sources* **181**(1), 140–143.

Kim, Y., Reed, D., Lee, Y.S., Lee, J.Y., Shim, J.H., Book, D. & Cho, Y.W. (2009). Identification of the dehydrogenated product of $Ca(BH_4)_2$. *J Phys Chem C* **113**(14), 5865–5871.

Kim, Y., Reed, D., Lee, Y.-S., Shim, J.-H., Han, H.N., Book, D. & Cho, Y.W. (2010). Hydrogenation reaction of CaH_2–CaB_6–Mg mixture. *J Alloy Compd* **492**(1–2), 597–600.

Orimo, S.I., Nakamori, Y., Eliseo, J.R., Zuttel, A. & Jensen, C.M. (2007). Complex hydrides for hydrogen storage. *Chem Rev* **107**(10), 4111–4132.

Rongeat, C., D'Anna, V., Hagemann, H., Borgschulte, A., Züttel, A., Schultz, L. & Gutfleisch, O. (2010). Effect of additives on the synthesis and reversibility of $Ca(BH_4)_2$. *J Alloy Compd* **493**(1–2), 281–287.

Vajo, J.J., Skeith, S.L. & Mertens, F. (2005). Reversible storage of hydrogen in destabilized $LiBH_4$. *J Phys Chem B* **109**(9), 3719–3722.

https://doi.org/10.1017/S1431927613012531 Published online by Cambridge University Press